

Supplementary Information: Quantum spin Hall phase transitions in two-dimensional SbBi alloy films

Wei-xiao Ji,* Chang-wen Zhang,† Meng Ding, Ping Li, and Pei-ji Wang
School of Physics and Technology, University of Jinan, Jinan, Shandong, 250022, P. R. China

I. STRUCTURES

The geometric and band information of buckled $\text{Bi}_x\text{Sb}_{8-x}$ and puckered $\text{Bi}_x\text{Sb}_{4-x}$ bilayers is given in Table S1.

II. COMPUTATIONS ON Z_2 TOPOLOGICAL INVARIANT

Z_2 topological invariant is calculated to identify QSH effects. Here we employ a recently proposed method for Z_2 index based on the $U(2N)$ non-Abelian Berry connection by Yu *et al.*¹. In this method, each state of the n -th occupied band is indexed by $|n, k_x, k_y\rangle$, and a square matrix $F(k_x, k_y)$ containing the overlap integrals

$$[F(k_x, k_y)]_{mn} = \langle m, k_{x,i}, k_y | n, k_{x,i+1}, k_y \rangle, \quad (1)$$

is defined. Then we calculate the complex unitary square matrix

$$D(k_y) = \prod_{j=0}^{N_x-1} F(j\Delta k_x, k_y), \quad (2)$$

whose complex eigenvalues $\lambda(k_y)$ have phase angle θ . Here $\Delta k_x = \frac{2\pi}{N_x a}$ is the discrete spacing of N_x points along k_x direction. Finally the Z_2 invariant is calculated

by counting the even or odd number of crossings of any arbitrary horizontal reference line with the evolution of $\theta, \text{mod } 2$. The Wannier center evolutions of buckled (5a), (5b) and (6a) are shown in Figure S1, in which the arbitrary reference line cross the evolution line an odd times for (5b) and (6a), indicating clearly $Z_2 = 1$.

III. COMPUTATIONS ON TOPOLOGICAL EDGE STATES

Also we calculate the edge states of semi-infinite buckled (6a), (5a), (5b) and (4a), and plot them in Figure S2, S3, S4 and S5 respectively. The number of edge states crossing the fermi level (red lines) shows that (6a) and (5b) are TIs while (5a) and (4a) are NIs. And it is found that the edge components are independent to their topological natures.

IV. SIMULATIONS OF MOLECULAR DYNAMICS AT ROOM TEMPERATURE

Ab initio molecular dynamics (MD) calculations at room temperature (300K) are performed using The Verlet algorithm is used where Newton's equations are integrated with time steps of 1fs. And a Nosè thermostat is used here. The stabilities of these SbBi alloy films are all maintained at room temperature (300K) as depicted from the MD snapshots of atomic structure in Figure S6.

* hellojiweixiao@163.com

† zhchwsd@163.com

¹ R. Yu, X. L. Qi, A. Bernevig, Z. Fang, and X. Dai, Physical Review B **84**, 075119 (2011).

TABLE S1. Geometry of buckled $\text{Bi}_x\text{Sb}_{8-x}$ and puckered $\text{Bi}_x\text{Sb}_{4-x}$ bilayers, where a and b are lattice constants, h is the averaged buckling distance, E_b is the binding energy, E_g and E_g^Γ are the global and Γ -point energy band gap, and the last column gives the space and point groups that all the configurations belong to.

Models		$a(\text{\AA})$	$b(\text{\AA})$	$h(\text{\AA})$	$E_b(\text{eV})$	$E_g(\text{meV})$	$E_g^\Gamma(\text{meV})$	Symmetry
Bi_8	(8a)	8.67	8.67	1.74	-2.444	506	587	$P\bar{3}m1(D_{3d}^3)$
Bi_7Sb_1	(7a)	8.62	8.62	1.74	-2.463	373	380	$P3m1(C_{3v}^1)$
Bi_6Sb_2	(6a)	8.57	8.57	1.74	-2.485	131	131	$P\bar{3}m1(D_{3d}^3)$
	(6b)	8.56	8.56	1.74	-2.485	206	206	$C2/m(C_{2h}^3)$
	(6c)	8.57	8.57	1.75	-2.483	153	155	$Pm(C_s^1)$
Bi_5Sb_3	(5a)	8.52	8.51	1.76	-2.507	63	63	$Cm(C_s^3)$
	(5b)	8.51	8.52	1.77	-2.507	11	11	$Cm(C_s^3)$
	(5c)	8.52	8.52	1.75	-2.504	95	95	$P3m1(C_{3v}^1)$
Bi_4Sb_4	(4a)	8.44	8.46	1.78	-2.530	157	157	$P21/m(C_{2h}^2)$
	(4b)	8.45	8.46	1.76	-2.528	286	286	$Cm(C_s^3)$
	(4c)	8.45	8.45	1.78	-2.528	222	222	$P3m1(C_{3v}^1)$
	(4d)	8.47	8.47	1.69	-2.523	367	378	$P3m1(C_{3v}^1)$
Bi_3Sb_5	(3a)	8.40	8.41	1.76	-2.553	506	506	$Cm(C_s^3)$
	(3b)	8.40	8.39	1.79	-2.552	434	434	$Cm(C_s^3)$
	(3c)	8.41	8.41	1.71	-2.549	541	548	$P3m1(C_{3v}^1)$
Bi_2Sb_6	(2a)	8.35	8.35	1.76	-2.577	756	756	$P\bar{3}m1(D_{3d}^3)$
	(2b)	8.35	8.34	1.81	-2.576	677	677	$C2/m(C_{2h}^3)$
	(2c)	8.35	8.35	1.70	-2.575	737	742	$Pm(C_s^1)$
Bi_1Sb_7	(1a)	8.29	8.29	1.72	-2.478	814	962	$P3m1(C_{3v}^1)$
Sb_8	(0a)	8.27	8.27	1.64	-2.338	1033	1212	$P\bar{3}m1(D_{3d}^3)$
Bi_4	(4a)	4.74	4.43	3.01	-2.440	106	288	$Pmna(D_{2h}^7)$
Bi_3Sb_1	(3a)	4.81	4.53	3.02	-2.490	298	859	$Pm(C_s^1)$
Bi_2Sb_2	(2a)	4.78	4.48	2.94	-2.535	316	1012	$Pmn21(C_{2v}^7)$
	(2b)	4.79	4.48	2.84	-2.534	186	885	$Pm(C_s^1)$
	(2c)	4.85	4.46	2.91	-2.519	243	845	$Pm(C_s^1)$
Bi_1Sb_3	(1a)	4.79	4.41	2.92	-2.572	274	887	$Pm(C_s^1)$
Sb_4	(0a)	4.81	4.53	2.83	-2.616	211	1026	$Pmna(D_{2h}^7)$

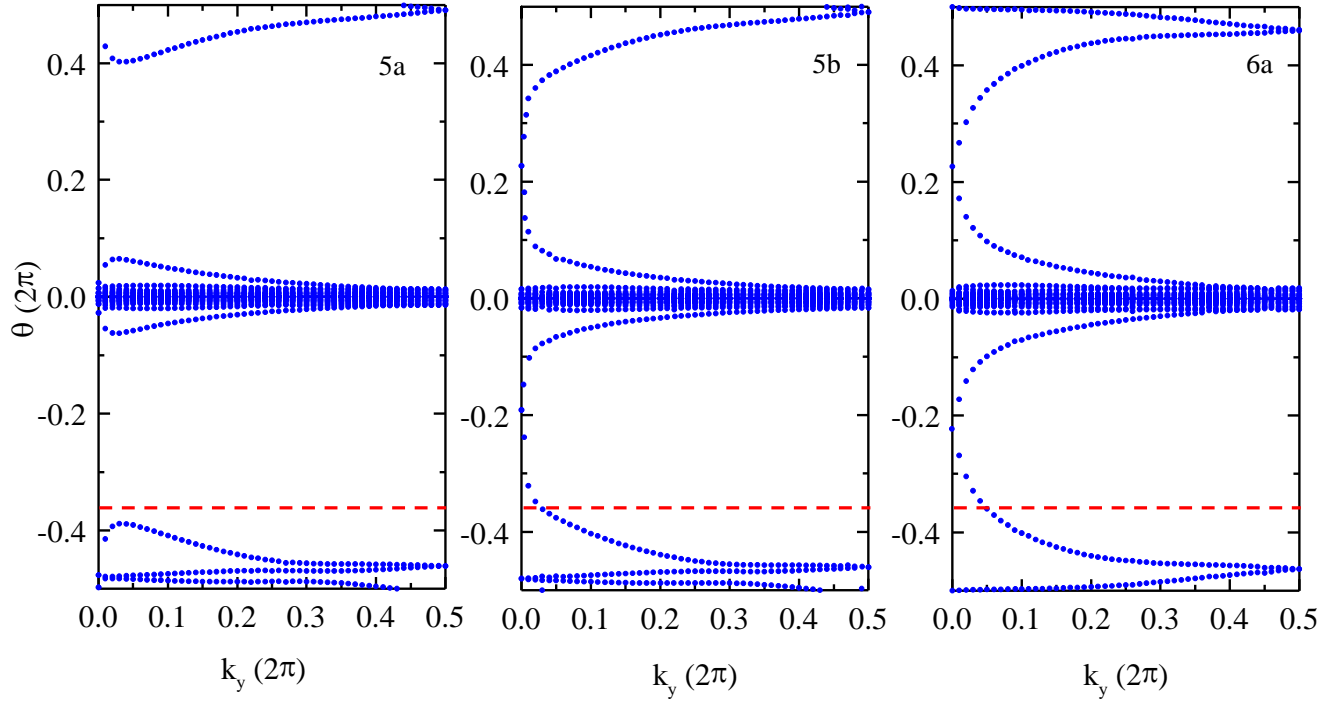


FIG. S1. The evolutions of Wannier centers of buckled (6a), (5a) and (5b). The parities of crossing points between blue curves and red reference lines are used to determine the Z_2 invariant.

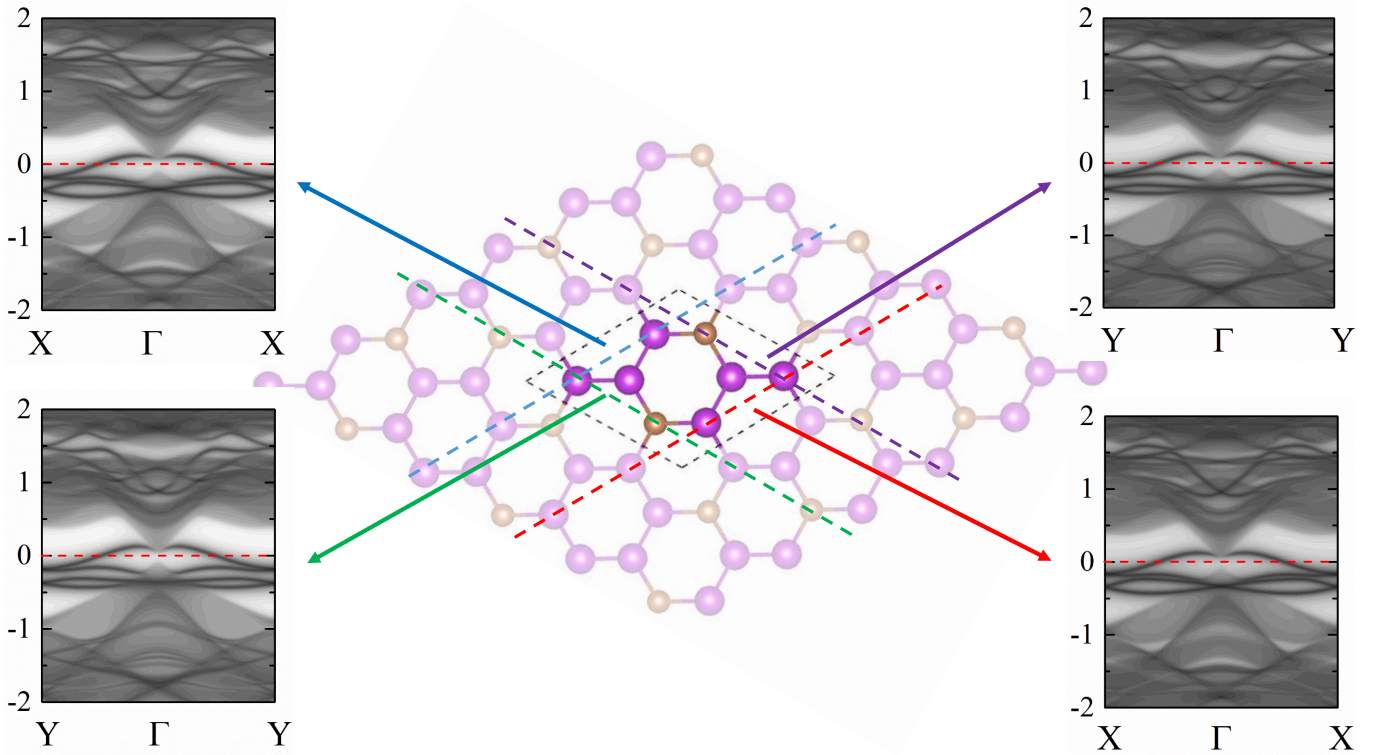


FIG. S2. The edge density of states of buckled $\text{Bi}_6\text{Sb}_2(\text{a})$.

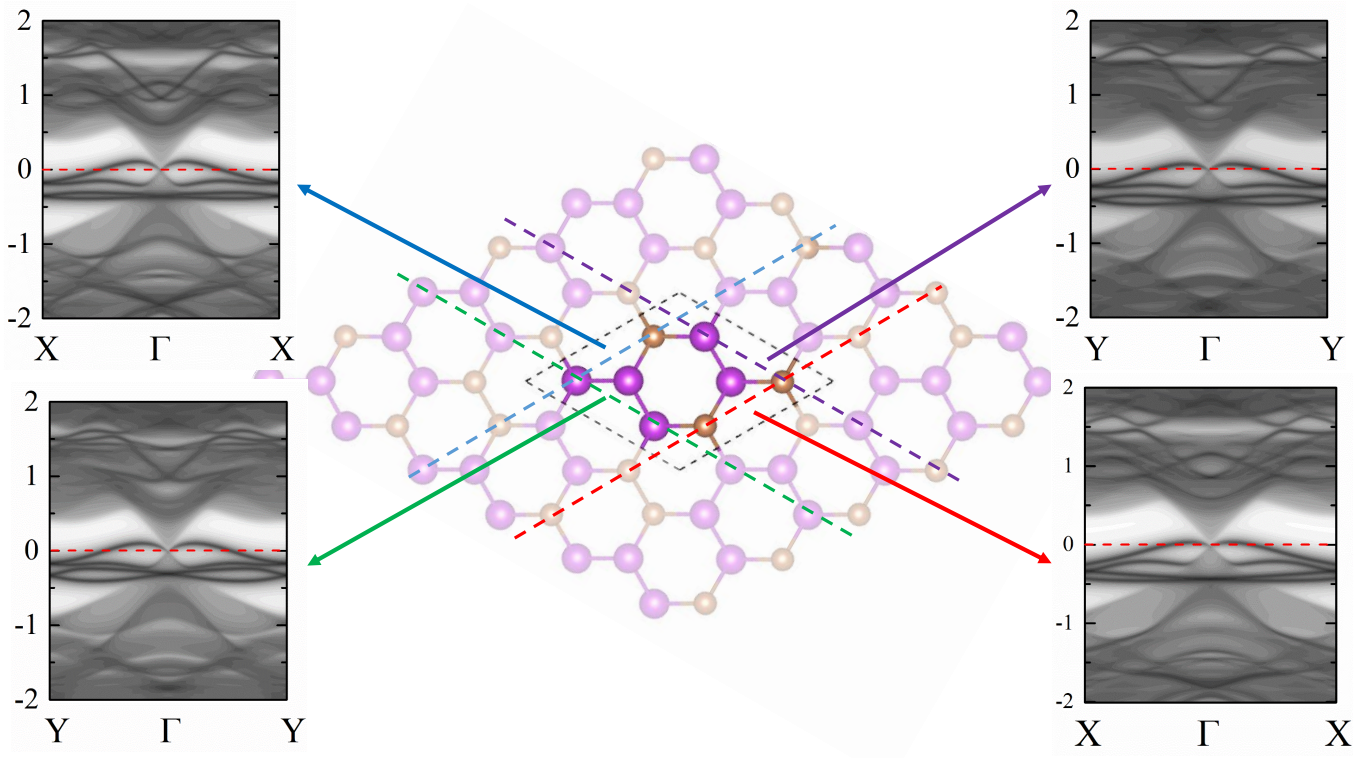


FIG. S3. The edge density of states of buckled Bi_5Sb_3 (a).

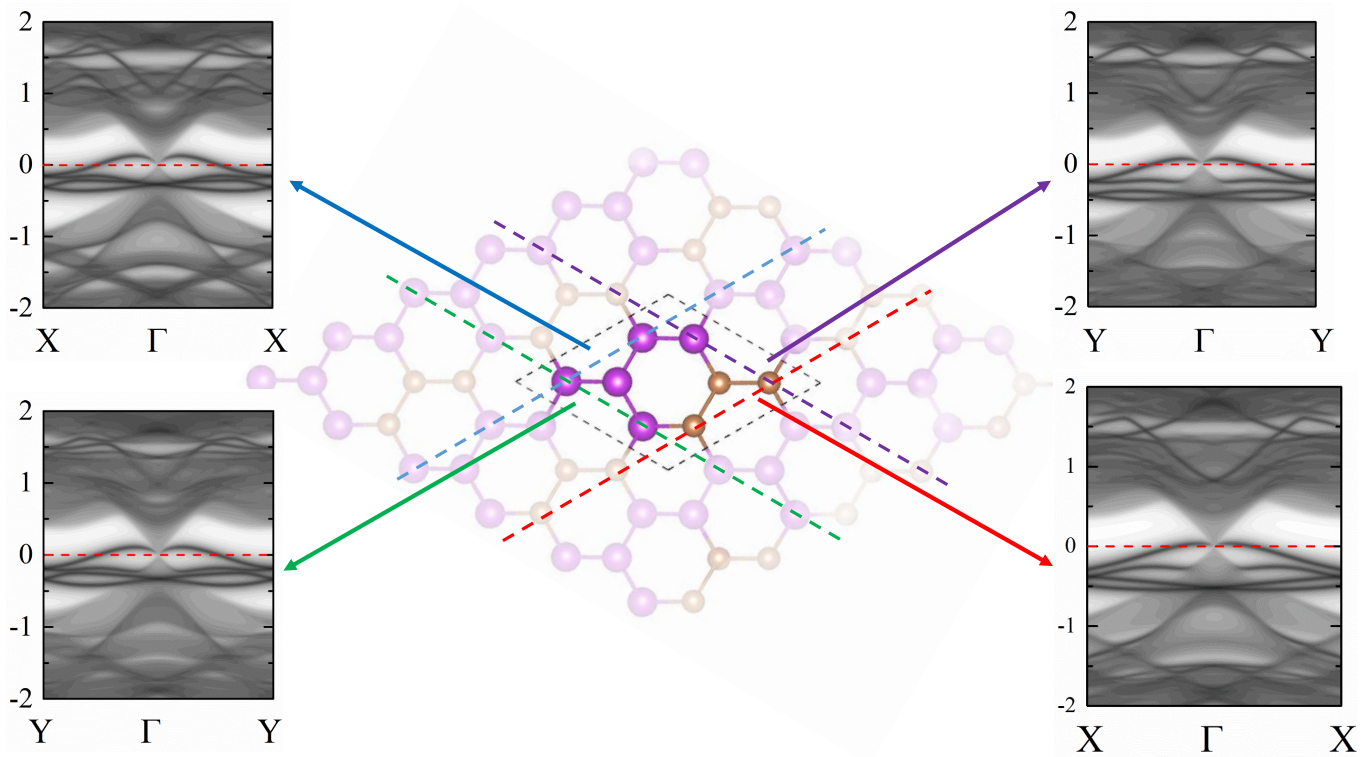


FIG. S4. The edge density of states of buckled Bi_5Sb_3 (b).

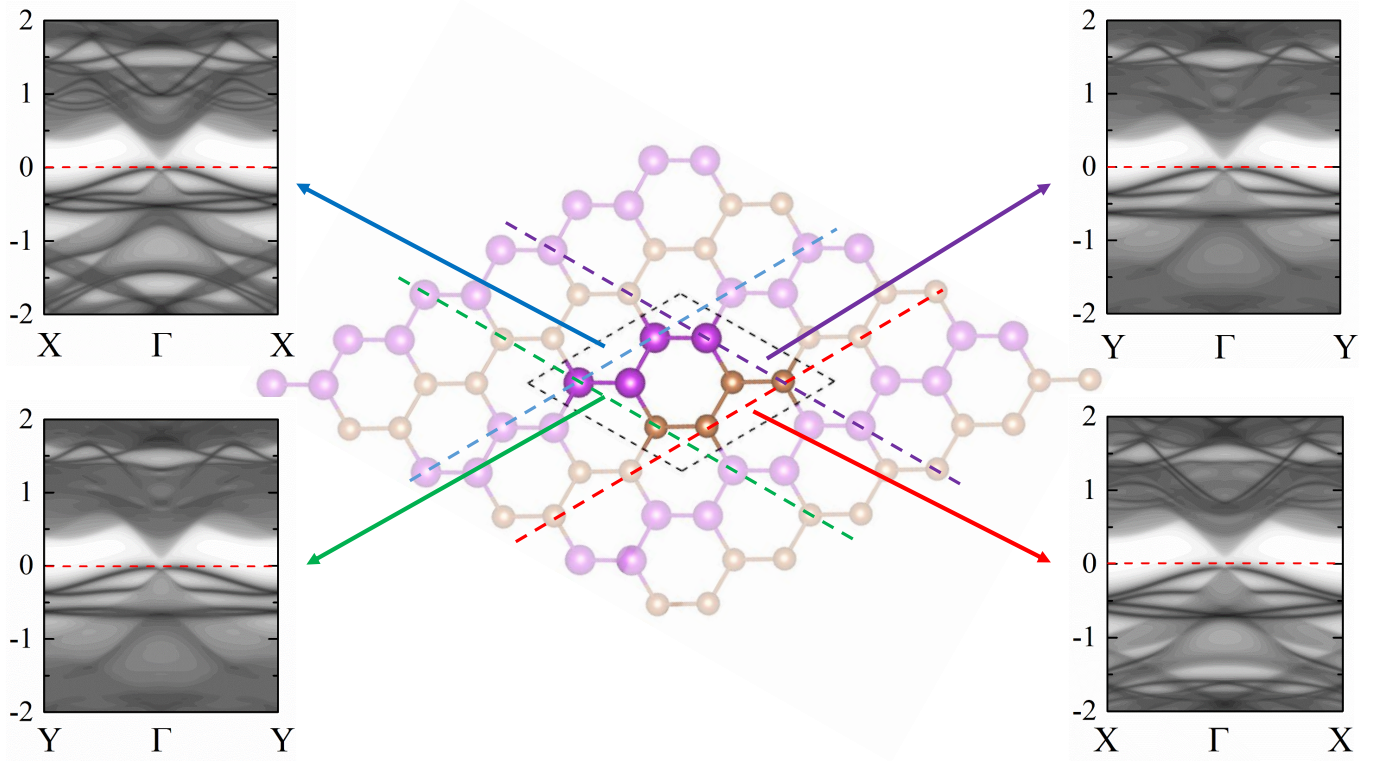


FIG. S5. The edge density of states of buckled Bi_4Sb_4 (a).

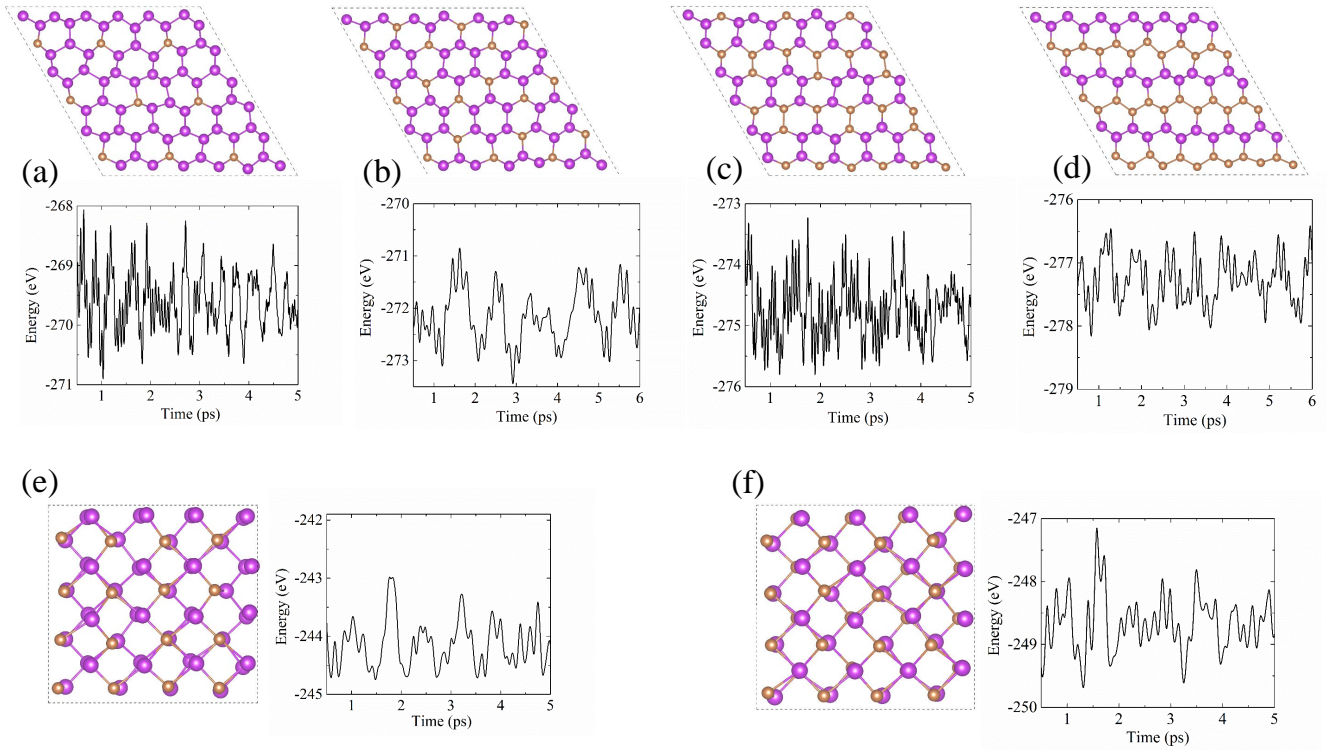


FIG. S6. Snapshots of atomic structure and energy evolutions calculated using *ab initio* MD calculations carried out at 300K.